

BRAIN COMMUNICATIONS

Chronic pain as a brain imbalance between pain input and pain suppression

Sven Vanneste¹ and Dirk De Ridder²

Chronic pain is pain that persists beyond the expected period of healing. The subjective experience of chronic pain results from pathological brain network interactions, rather than from persisting physiological sensory input of nociceptors. We hypothesize that pain is an imbalance between pain evoking dorsal anterior cingulate cortex and somatosensory cortex and pain suppression (i.e. pregenual anterior cingulate cortex). This imbalance can be measured objectively by current density ratios between pain input and pain inhibition. A balance between areas involved in pain input and pain suppression requires communication, which can be objectively identified by connectivity measures, both functional and effective connectivity. In patients with chronic neuropathic pain, electroencephalography is performed with source localization demonstrating that pain is reflected by an abnormal ratio between the dorsal anterior cingulate cortex, somatosensory cortex and pregenual anterior cingulate cortex. Functional connectivity demonstrates decreased communication between these areas, and effective connectivity puts the culprit at the dorsal anterior cingulate cortex, suggesting that the problem is related to abnormal behavioral relevance attached to the pain. In conclusion, chronic pain can be considered as an imbalance between pain input and pain suppression.

1 Global Brain Health Institute, Institute of Neuroscience, Trinity College Dublin, Dublin, Ireland

2 Department of Surgical Sciences, Section of Neurosurgery, Dunedin School of Medicine, University of Otago, 9016 Dunedin, New Zealand

Correspondence to: Sven Vanneste

Lab for Clinical & Integrative Neuroscience, Global Brain Health Institute and Institute of Neuroscience, Trinity College Dublin, College Green 2, Dublin, Ireland.

E-mail: sven.vanneste@tcd.ie website: <http://www.lab-clint.org>

Keywords: pain; medial pathway; lateral pathway; descending pathway; anterior cingulate cortex

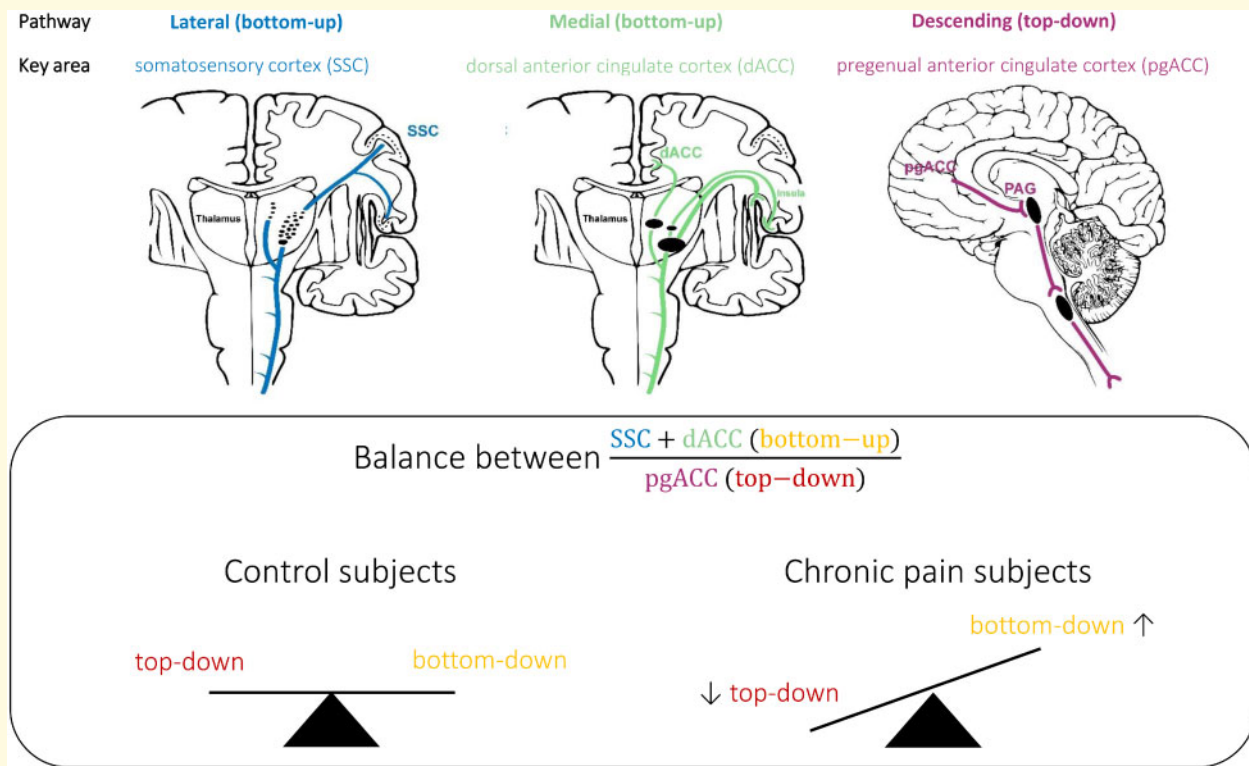
Abbreviations: ADHD = Attention Deficit Hyperactivity Disorder; dACC = dorsal anterior cingulate cortex; EEG = electroencephalogram; FRP = false positive rate; MAE = mean absolute error; MRI = magnetic resonance imaging; NRS = numeric rating scale; pgACC = pregenual anterior cingulate cortex; PVAQ = pain vigilance and awareness questionnaire; RMSE = root mean squared error; ROC = relative operating characteristic curve; sLORETA = standardized low-resolution brain electromagnetic tomography; SSC = somatosensory cortex; SVM = support vector machine; TPR = true positive rate

Received July 06, 2020. Revised November 19, 2020. Accepted November 23, 2020. Advance Access publication February 16, 2021

© The Author(s) (2021). Published by Oxford University Press on behalf of the Guarantors of Brain.

This is an Open Access article distributed under the terms of the Creative Commons Attribution License (<http://creativecommons.org/licenses/by/4.0/>), which permits unrestricted reuse, distribution, and reproduction in any medium, provided the original work is properly cited.

Graphical Abstract



Introduction

Over one-third of the world's population suffers from persistent or chronic pain, resulting in tremendous burden for the individual (Jensen *et al.*, 2014) and society (Gaskin and Richard, 2012). The subjective experience of chronic pain results from pathological brain network interactions, rather than from persisting physiological sensory input via nociceptors (Jensen *et al.*, 2014). Pain is processed by three known pathways (Rainville *et al.*, 1997; Price, 2000; Fields, 2004; Eippert *et al.*, 2009; Kong *et al.*, 2010; De Ridder and Vanneste, 2016). The two ascending pathways include the anatomically and functionally separable medial and lateral pain pathway (Price, 2000; Bushnell *et al.*, 2013). The medial pain pathway, which involves the dorsal anterior cingulate cortex (dACC) and anterior insula as main hubs, encodes the unpleasantness and suffering of pain (Rainville *et al.*, 1997; Price, 2000; Bushnell *et al.*, 2013). The lateral pathway, which involves the somatosensory cortex (SSC) as major hub, processes the discriminatory/sensory components of the pain (Flor *et al.*, 1995; Bushnell *et al.*, 2013). In addition, a descending pain inhibitory pathway (Fields, 2004) involves the rostral and pregenual anterior cingulate cortex (pgACC), the periaqueductal gray, hypothalamus and rostral ventromedial brainstem (Fields 2004; Eippert *et al.*, 2009; Kong *et al.*, 2010). This descending pathway is responsible for stress-mediated

pain inhibition (Yilmaz *et al.*, 2010), and placebo analgesia (Eippert *et al.*, 2009).

It has been proposed that pain is the result of an imbalance between brain areas that process pain input and pain suppression (De Ridder and Vanneste, 2016), and that if pain input equals pain suppression there is no pain perception, but if pain input is larger than pain suppression this results in subjective pain perception (De Ridder and Vanneste, 2016). This imbalance can be computed by analyzing the current density of the different frequency bands of the electroencephalogram (EEG) spectrum, source localized to the pgACC, dACC and SSC (De Ridder and Vanneste, 2016).

The frequency bands of interest within the EEG spectrum are θ , α and γ band activity, based on the thalamocortical dysrhythmia model of pain (Llinas *et al.*, 1999; Sarnthein *et al.*, 2005; Stern *et al.*, 2006; Cauda *et al.*, 2009; Walton *et al.*, 2010; De Ridder *et al.*, 2011; Schulman *et al.*, 2011; Sametsky *et al.*, 2015; Vanneste *et al.*, 2018). The thalamocortical dysrhythmia hypothesis suggests that somatosensory deafferentation leads to a thalamocortical column-specific decrease in information processing, which permits slowing down of resting-state thalamocortical activity from normal α to the θ frequency range (Llinas *et al.*, 1999, 2005; Vanneste *et al.*, 2018). Decreased input also results in a reduction of GABA_A-mediated lateral inhibition, inducing γ band activity surrounding the deafferented thalamocortical columns

(Llinas *et al.*, 2005). This γ band activity surrounding θ activity is known as the edge effect (Llinas *et al.*, 1999, 2005). An abnormal increase of θ oscillations in chronic pain patients has been identified (Sarnthein *et al.*, 2006; Stern *et al.*, 2006). Other studies, however, did not observe abnormal θ oscillations in chronic pain (Schmidt *et al.*, 2012; Jensen *et al.*, 2013), but only a slowing of the peak α frequency in chronic pain (de Vries *et al.*, 2013). Furthermore, abnormal θ oscillations might basically represent the non-specific slowing of α activity observed in many chronic neurological and psychiatric disorders (Vanneste *et al.*, 2018).

It has been proposed that the θ - γ coupling in thalamocortical dysrhythmia represents pain-related γ activity (Babiloni *et al.*, 2002) nested on θ as a carrier wave (Lisman and Jensen, 2013), analogous to what has been proposed for cognitive processing (Canolty *et al.*, 2006). This γ activity nested on θ is also known in other pathologies such as tinnitus, depression, Parkinson's disease, addiction, ADHD, etc. (Coullaut-Valera *et al.*, 2014; De Ridder *et al.*, 2015; Kim *et al.*, 2015, 2017; Mumtaz *et al.*, 2017; Vanneste *et al.*, 2018).

A balance between pain input and pain suppression requires communication between the involved areas. Communication in the brain can be analyzed by functional connectivity, effective connectivity and cross-frequency coupling. Functional connectivity reflects correlated activity between two or more areas in the brain, effective connectivity adds directionality to the functional connectivity and cross-frequency coupling looks at how high frequency activity (β and γ) is nested on low frequency activity (δ , θ , α).

This study wants to confirm or disprove the proposed brain imbalance model for pain using EEG to analyze source localized activity (=current density) and connectivity. Based on the thalamocortical dysrhythmia model for pain the frequencies of interest are θ , α and γ , the regions of interest are the main hubs of the lateral pathway (=SSC), the medial pathway (=dACC) and descending pain inhibitory pathway (=pgACC). We hypothesize that pain is associated with an increased ratio >1 of the current density of (dACC+SSC)/2 \times pgACC, that the functional and effective connectivity is disrupted in the θ and α band, and the cross-frequency coupling abnormal in θ - γ .

Methods and materials

Participants

This study consists of 100 subjects (50 women and 50 men; 34–66 years of age, $M=48.47$; $SD = 11.04$): 50 healthy control subjects, and 50 subjects with chronic pain. The healthy control group reported no history of neurological or neuropsychiatric disorders, and no pain. A pain specialist screened the pain patients for

neuropathic pain related to deafferentation (i.e. peripheral nerve, root, or central tract lesions). Whereas traditionally chronic pain is defined as pain lasting for more than 3 months (Treede *et al.*, 2015), the patients in this study suffered pain for more than one year.

The pain score (pain percept: how severe is your pain?) on a numeric rating scale was 5.80 ($SD = 2.57$) and on the pain vigilance and awareness questionnaire (PVAQ) 47.01 ($SD = 9.41$). The PVAQ is a measurement that assesses the preoccupation with or attention to pain and pain changes, and is associated with pain-related fear and perceived pain severity (Roelofs *et al.*, 2003). The study was in accordance with the ethical standards of the Helsinki declaration (1964) and was approved by the institutional ethics committee (UZA OGA85). All relevant data are available from the authors on request.

Electroencephalogram

Recordings

EEG data (Neuroscan, <http://compumedicsneuroscan.com/>) were obtained in a quiet room while each participant was sitting upright on a comfortable chair. The EEG was recorded with 64 electrodes in the standard 10–10 International placement. The impedances were checked to remain below 5 k Ω . Data recording was eyes-closed (sampling rate = 1 kHz, band passed DC–200 Hz) and lasted approximately 5 min. The ground electrode was located at AFZ and the reference was located at the vertex. Participants were instructed not to drink caffeinated beverages one hour and alcohol 24 hours prior before recording to avoid alcohol- or caffeine-induced changes in the EEG stream (Volkow *et al.*, 2000; Logan *et al.*, 2002; Siepmann and Kirch, 2002). By monitoring both slowing of the alpha rhythm and appearance of spindles in the EEG stream we checked the alertness of participants to prevent possible enhancement of the θ power due to drowsiness during recording (Moazami-Goudarzi *et al.*, 2010). Our data were resampled to 128 Hz, band-pass filtered in the range 2–44 Hz, plotted and carefully inspected for manual artifact-rejection. We removed all episodic artifacts including eye blinks, eye movements, teeth clenching, body movement, or ECG artifact from the stream of the EEG. We computed the average Fourier cross-spectral matrices for frequency bands δ (2–3.5 Hz), θ (4–7.5 Hz), α (8–12 Hz), β (13–30 Hz) and γ (30.5–44 Hz).

Source localization analysis

Standardized low-resolution brain electromagnetic tomography (sLORETA, available at <http://www.uzh.ch/keyinst/loreta.htm>) is a method for functional imaging yielding standardized current density with zero localization error based on certain electrophysiological and neuroanatomical constraints (Pascual-Marqui, 2002). This method is developed to estimate the intracerebral sources generating the scalp-recorded electrical activity in the five frequency bands defined (Song *et al.*, 2015). The sLORETA

algorithm solves the inverse problem by assuming related orientations and strengths of neighboring neuronal sources that are represented by adjacent voxels. The solution space used in this study and associated lead field matrix are those implemented in the LORETA-Key software. By applying the boundary element method on the MNI-152 (Montreal Neurological Institute, Canada) sLORETA implements revisited realistic electrode coordinates (Jurcak *et al.*, 2007) and the lead field (Fuchs *et al.*, 2002) on a MNI-152 volume with 6239 voxels together with a size of $5 \times 5 \times 5$ mm. The co-registration makes use of the correct translation from the MNI-152 space into the Talairach and Tournoux space.

Region of interest analysis

The log-transformed electric current density was calculated for each regions of interest (ROIs) and averaged across all voxels belonging to the ROI for the five frequency bands included in this study. The ROIs in the present study are the left and right SSC, the dACC, and pgACC. We did not differentiate between left and right dACC, pgACC due to their proximity to the midline, as due to volume conduction, laterality is harder to differentiate for areas close to the midline.

Support vector machine

We used the SVM program in the data-mining software Weka to perform all classification tasks (Waikato Environment for Knowledge Analysis version 3.7, developed by the University of Waikato Machine Learning Group, available at <http://www.cs.waikato.ac.nz/ml/weka/>) (Smith and Frank, 2016) We build a predictive models by learning from examples provided in user supplied datasets and used the default settings as the running parameters. Our dataset included for each participant the five frequency bands for each ROI. The criterion for correct classification was defined by subjects being assigned to the correct group (e.g. for the full model: disorder versus healthy). The classification method that was used, was a linear logistic regression-based classifier as the classification method. A 10-fold cross-validation was performed on the full dataset (see Vanneste *et al.*, 2018 for more detail information). The measurements of model accuracy calculated by the k -fold cross-validation technique include the true-positive ratio (TPR), false-positive ratio (FPR), root mean squared error (RMSE), mean average error (MAE), and κ -statistic (see Vanneste *et al.*, 2018 for more detail information about this specific measures). In order to determine significance of the model accuracy for pain/control, averaged model accuracy was calculated through randomization of the data. This was done by taking the same dataset used to generate the pain model and randomly reassigning patient data as either pain or control. This randomized dataset was then used to generate a prediction model and to model accuracy values. This was done 100 times, and the resulting randomized model accuracy statistics were averaged across all trials.

Lagged phase coherence

Phase coherence between time series corresponding to different spatial locations are usually interpreted as indicators of functional connectivity. Pascual-Marqui (2007a,b) introduced measures of coherence and phase synchronization that takes into account only non-instantaneous connectivity. Because this method the confounding factor of volume conduction is removed. The lagged phase coherence between two sources can then be interpreted as the amount communication between the regions contributing to the ROI defined. Since the two components oscillate coherently with a lag, the crosstalk can be interpreted as information sharing (more detail information can be found in Vanneste *et al.*, 2014).

Granger causality

Granger causality reflects information transfer strength also called effective connectivity. By quantifying how much the signal in the seed region is able to predict the signal in the target region we calculated the effective connectivity from one region to another (Granger, 1969; Geweke, 1982). Granger causality is defined as the log-ratio between the error variance of a reduced model, which predicts one time series based only on its own past values, and that of the full model, which in addition includes the past values of another time series. In this study, we look at the granger causality between the pgACC, dACC, and the left and right SSC.

Cross-frequency coupling

θ - β , θ - γ and α - γ coupling are proposed to be effective means of communication between cortically distant areas (Canolty *et al.*, 2006). To verify whether this is present, cross-frequency coupling was calculated for the pgACC, dACC, and the left and right SSC. Phase-amplitude was computed by computing the time-series for the x , y and z components of the current for each ROI. Next, these were filtered in the θ , α , β and γ frequency band-pass regions. For each ROI and each frequency band, a principal component analysis was calculated, and the first component was retained for the θ and γ bands. A Hilbert transform was then calculated on the gamma component and the signal envelope retained. Finally, the Pearson correlation between the θ/α component and the envelope of the β/γ envelope was computed for each participant.

Statistical analysis

Support vector machine

To compare the different outcome measures (correctly classified, incorrectly classified, TPR, FPR, ROC, κ -statistic, RMSE and MAE) of the SVM learning approach, we applied a univariate ANOVA with the model (test versus random) as the independent variable and the outcome measures as the dependent variable.

Region of interest

We performed a MANOVA including the log-transformed current density for the pgACC, dACC and the left and right SSC as dependent variables and group (chronic pain patients versus control subjects) as independent variables. These areas were selected based on the a priori hypothesis and were confirmed by SVM. For each area, we analyzed only the frequencies that showed up when applying in the SVM learning approach. Based on the outcome, a simple contrast analyses were conducted to look at specific effects for a specific frequency and a specific area. Pearson correlations were calculated between the region of interest and the pain score for the frequency bands at the areas that showed up during SVM. This analysis was corrected for pairwise comparisons using a Bonferroni correction. In addition, we looked at the balance between the areas that are part of the ascending pathway (i.e. dACC and the left/right SSC) and the descending pathway (i.e. pgACC). We include only the frequency bands that correlated with the pain percept as measured with the visual analogue scale. As the dACC and SSC combine two current densities and the pgACC only one, the current density of the pgACC was doubled, as such, the balance was calculated as follows:

$$\frac{\left(\beta |dACC + \frac{(\gamma |left\text{ SSC} + \gamma |right\text{ SSC})}{2} \right)}{\theta |pgACC}$$

If the balance was greater than one, then it suggests that the key areas involved in the ascending pathways are more active in comparison to the key area involved in the descending pathway. If the balance was less than one, then it suggests that the key areas involved in the ascending pathways are less active in comparison to the key area involved in the descending pathway. If the balance is similar to one, then the key areas involved in the ascending pathways are as active as the key area involved in the descending pathway. A univariate ANOVA was applied to compare the balance between the control subjects and the chronic pain patients. In addition, a Pearson correlation was applied between the pain percept and the balance score.

Lagged phase coherence or functional connectivity

A comparison was made between chronic pain patients versus control subjects for all frequency bands. The threshold of significance for a given lagged phase coherence can be found as described by Pascual-Marqui (2002, 2007a,b). Time-series of current density were extracted for different regions of interest using sLORETA. Power in all 6239 voxels was normalized to a power of 1 and log transformed at each time point. Region-of-interest values thus reflect the log transformed fraction of total power across all voxels, separately for specific frequencies. The regions of interest selected were the pgACC, dACC, and left and right SSC. Lagged phase synchronization/

coherence or functional connectivity contrast maps were calculated for all frequency bands: δ (2–3.5 Hz), θ (4–7.5 Hz), α (8–12 Hz), β (13–30 Hz) and γ (30.5–44 Hz). The significance threshold was based on a permutation test with 5000 permutations. This methodology corrects for multiple testing (i.e. for the collection of tests performed for all voxels, and for all frequency bands).

Granger causality

We applied Granger causality analysis to look at the direction of functional connectivity (i.e. effective connectivity). For the θ frequency, we performed a MANOVA including the Granger causality for the effective connectivity (pgACC→left SSC, left SSC→pgACC, pgACC→right SSC, and right SSC→pgACC) as dependent variables, and group (chronic pain patients versus control subjects) as independent variables. Based on the outcome, simple contrast analyses were conducted for the individual connections. For the alpha frequency, we performed a MANOVA including the effective connectivity (pgACC→left SSC, left SSC→pgACC, pgACC→right SSC, right SSC→pgACC, pgACC→dACC, dACC→pgACC, dACC→left SSC, left SSC→dACC, dACC→right SSC, right SSC→dACC, left SSC→right SSC and right SSC→left SSC) as dependent variables and group (chronic pain patients versus control subjects) as independent variables. Based on the outcome, simple contrast analyses were conducted for the individual connections. We calculated Pearson correlations between effective connectivity and pain perception for all connections that showed a significant group-level effect.

Cross-frequency coupling

We performed a MANOVA including θ - γ and α - γ phase-amplitude coupling for the both the left and right SSC and α - β coupling for the dACC as dependent variables and group (chronic pain patients versus control subjects) as independent variables. Based on the outcome, simple contrast analyses were conducted to look at specific effects. A Pearson correlation was computed between θ - γ and α - γ coupling for the left and right SSC for both the chronic pain patients and control subjects. Furthermore, a Pearson correlation was calculated between the phase-amplitude coupling for θ - γ and α - γ for the SSC, the α - β coupling for the dACC, and pain perception as well as the balance between θ - γ and α - γ for the SSC.

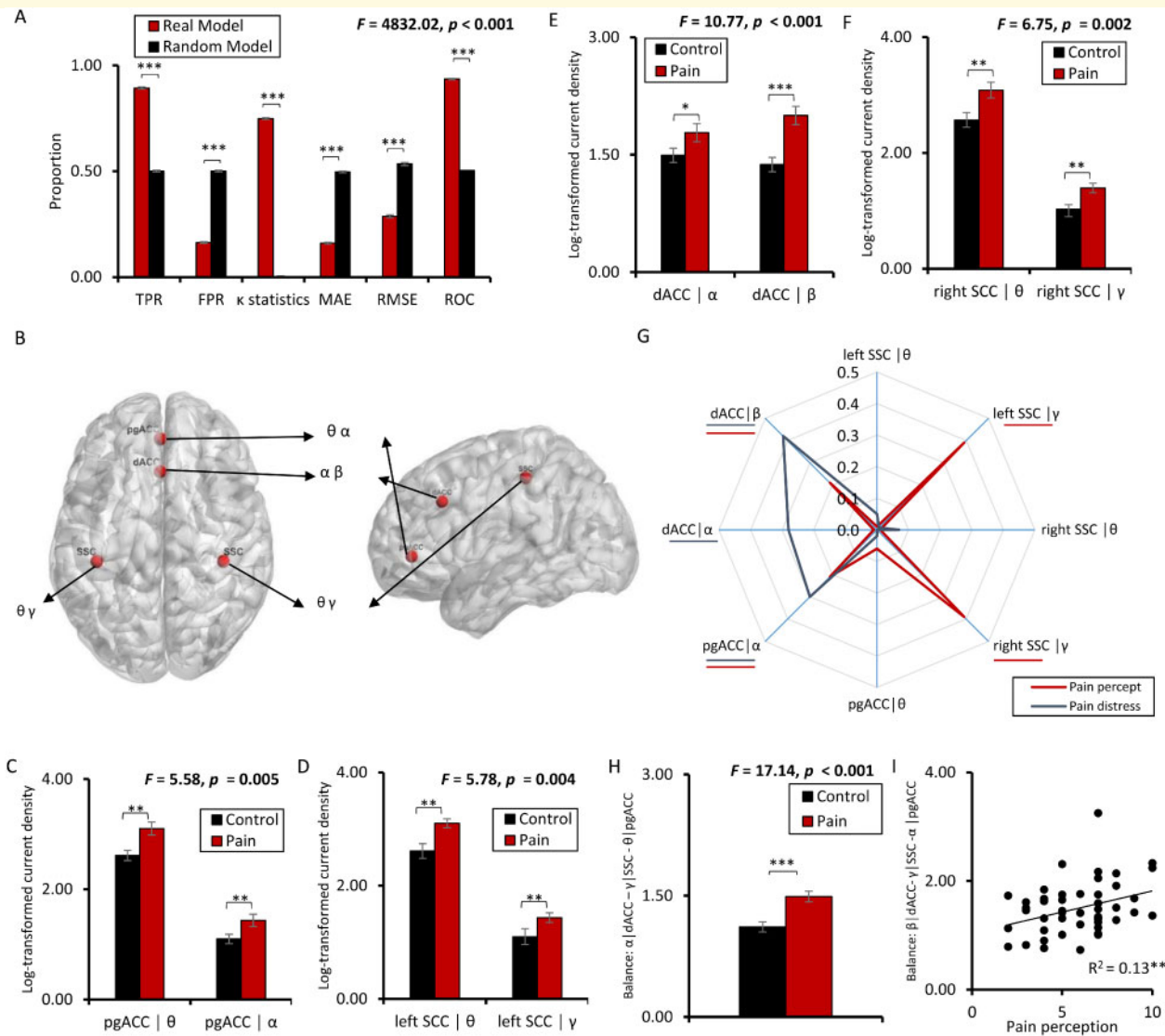
Data availability

Data will be made available upon reasonable request.

Results

Support vector machine learning

Using a SVM learning approach, chronic pain ($n=50$) can be objectively detected in comparison to pain-free



control subjects ($n=50$), solely based on brain activity of the dACC (including α and β band), the SSC (including θ and γ band), and the pgACC (including θ and α band) with an accuracy of 89.3%. The other frequency bands, namely delta and beta, were not selected by the model. A random model has an accuracy not higher than chance

(TPR: 50%) ($F=2593.09$, $P < 0.001$) (Fig. 1a, b). The FRP was significantly ($F=22772.37$, $P < 0.001$) lower for the pain model ($M = 0.16$, $SD = 0.02$) in comparison to the random model ($M = 0.50\%$, $SD = 0.02$). The area under the curve shows a significant effect ($F=7281.34$, $P < 0.001$), indicating a higher score for

the pain model ($M = 0.94$, $SD = 0.003$) in comparison to the random model ($M = 0.50$, $SD = 0.003$). A significant difference was also obtained by comparing the κ -statistic (pain: $M = 0.75$, $SD = 0.02$ versus random: $M = 0.002$, $SD = 0.004$; $F = 13404.91$, $P < 0.001$), MAE (pain: $M = 0.16$, $SD = 0.005$ versus random: $M = 0.50$, $SD = 0.005$; $F = 2299.95$, $P < 0.001$), and RMSE (pain: $M = 0.29$, $SD = 0.007$ versus random: $M = 0.54$, $SD = 0.007$; $F = 436.24$, $P < 0.001$) (Fig. 1a, b). For the areas individually, the maximum accuracy was 68.8% (dACC: 67.4%; the SSC: 68.8%; pgACC: 63.3%) and the accuracy for the dACC and SSC together was 79.3%, confirming that pain can better be explained by looking at the pain input and suppression areas together (89.3% accuracy), i.e. as a balance.

Region of interest

A region of interest analysis further shows that chronic pain is the result of an increase in activity in the SSC (θ and γ band; left: $F = 5.78$, $P = 0.004$; right: $F = 6.75$, $P = 0.002$), dACC (α and β band; $F = 10.77$, $P < 0.001$), and pgACC (θ and α band; $F = 5.58$, $P = 0.005$) (Fig. 1c–f). These effects remained after correction for multiple comparison using a Bonferroni correction ($P < 0.016$). A significant increase for the pain patients in the left (θ : $M = 3.10$, $SD = 1.06$, $F = 6.48$, $P = 0.010$; γ : $M = 1.43$, $SD = 0.72$, $F = 8.36$, $P = 0.005$) and right SCC (θ : $M = 3.08$, $SD = 1.01$, $F = 7.82$, $P = 0.006$; γ : $M = 1.40$, $SD = 0.67$, $F = 10.29$, $P = 0.002$) was obtained in comparison to the control group (left SCC for θ : $M = 2.61$, $SD = 0.92$; and for γ : $M = 1.010$, $SD = 0.48$ and right SCC for θ : $M = 2.57$, $SD = 0.90$; for γ : $M = 1.02$, $SD = 0.50$), respectively. For the pgACC, both for the θ and α band a significant increase in current density was identified for pain patients (θ : $M = 3.10$, $SD = 0.89$, $F = 7.64$, $P = 0.009$; α : $M = 1.44$, $SD = 0.84$, $F = 8.13$, $P = 0.005$) in comparison to the control subjects (θ : $M = 2.61$, $SD = 0.65$; α : $M = 1.10$, $SD = 0.61$). Also, a comparison between the current density for the dACC for the α and β band revealed a significant increase for the pain patients (α : $M = 1.78$, $SD = 0.87$, $F = 5.53$, $P = 0.039$; β : $M = 2.01$, $SD = 0.86$, $F = 13.25$, $P < 0.001$) in comparison to the control subjects (α : $M = 1.49$, $SD = 0.63$; β : $M = 1.37$, $SD = 0.64$). These effects remained after correction for multiple comparison using a Bonferroni correction ($P < 0.0125$).

The current density correlates with the pain percept in γ for left SSC (γ : $R^2 = 0.39$, $P < 0.001$) and right SSC (γ : $R^2 = 0.39$, $P < 0.001$), in β for the dACC (β : $R^2 = 0.21$, $P = 0.007$) and alpha for pgACC (α : $R^2 = 0.21$, $P = 0.007$), but not for θ , neither in the left SSC (θ : $R^2 = 0.01$, $P = 0.46$), right SSC (θ : $R^2 = 0.01$, $P = 0.65$), nor pgACC (θ : $R^2 = 0.06$, $P = 0.43$), and neither for α in the dACC (α : $R^2 = 0.01$, $P = 0.08$) (Fig. 1g). These effects continued after correction for multiple comparison using a Bonferroni correction ($P < 0.008$).

A correlation analysis was performed between the current density and pain severity/distress as measured by the pain vigilance and awareness questionnaire. This analysis revealed a significant positive correlation between the current density in α in the pgACC (α : $R^2 = 0.30$, $P < 0.001$) and α and β in the dACC (α : $R^2 = 0.28$, $P < 0.001$; β : $R^2 = 0.42$, $P < 0.001$) indicating the higher the score for pain related distress, the higher the current density, or vice versa. No effect was obtained for left SSC (θ : $R^2 = 0.05$, $P = 0.32$; γ : $R^2 = 0.01$, $P = 0.37$) and right SSC (θ : $R^2 = 0.07$, $P = 0.07$; γ : $R^2 = 0.001$, $P = 0.87$) and the pgACC (θ : $R^2 = 0.02$, $P = 0.26$) (Fig. 1g). The effects continued after correction for multiple comparison using a Bonferroni correction ($P < 0.008$).

The balance between the areas of interest (pgACC, dACC and SSC) is significantly different from healthy pain-free subjects ($F = 17.14$, $P < 0.001$) and furthermore correlates with intensity of the pain ($R^2 = 0.13$, $P = 0.012$) (Fig. 1h–i). No correlation was obtained between the balance between these significant areas and pain distress ($R^2 = 0.07$, $P = 0.08$). After correction for multiple comparisons using a Bonferroni correction the effects remained ($P < 0.025$).

Functional connectivity

Functional connectivity, based on lagged phase synchronization between the ROI brain areas demonstrates that chronic pain patients have decreased functional connectivity in the α band ($t = 3.94$, $P < 0.05$) and more functional connectivity in the θ band ($t = 4.81$, $P < 0.05$) (Fig. 2). No effect was obtained for δ , β and γ bands.

Effective connectivity

For the θ band, an overall effect for effective connectivity as measured with Granger causality between the pgACC and the SSC ($F = 4.09$, $P < 0.004$); Fig. 3a–c) was overall identified. A post-hoc univariate ANOVA revealed that there is less information sent from the pgACC to the left ($M = 0.013$, $SD = 0.008$; $F = 4.87$, $P = 0.041$) and right SSC ($M = 0.012$, $SD = 0.008$; $F = 4.12$, $P = 0.045$) for pain patients in comparison to the control subjects (left $M = 0.016$, $SD = 0.008$; right: $M = 0.016$, $SD = 0.009$). Increased information is transferred from both the left ($M = 0.02$, $SD = 0.009$; $F = 11.36$, $P < 0.001$) and right SSC ($M = 0.020$, $SD = 0.011$; $F = 6.56$, $P = 0.012$) to the pgACC for patients in comparison to control subjects (left $M = 0.014$, $SD = 0.008$; right: $M = 0.015$, $SD = 0.009$).

In patients with chronic pain both the information that is sent from pgACC to the left ($R^2 = 0.11$, $P = 0.042$) and right SSC ($R^2 = 0.11$, $P = 0.041$) negatively correlates with pain perception, as measured by the NRS. These effects, however, did not remain after correction for multiple comparison using a Bonferroni correction,

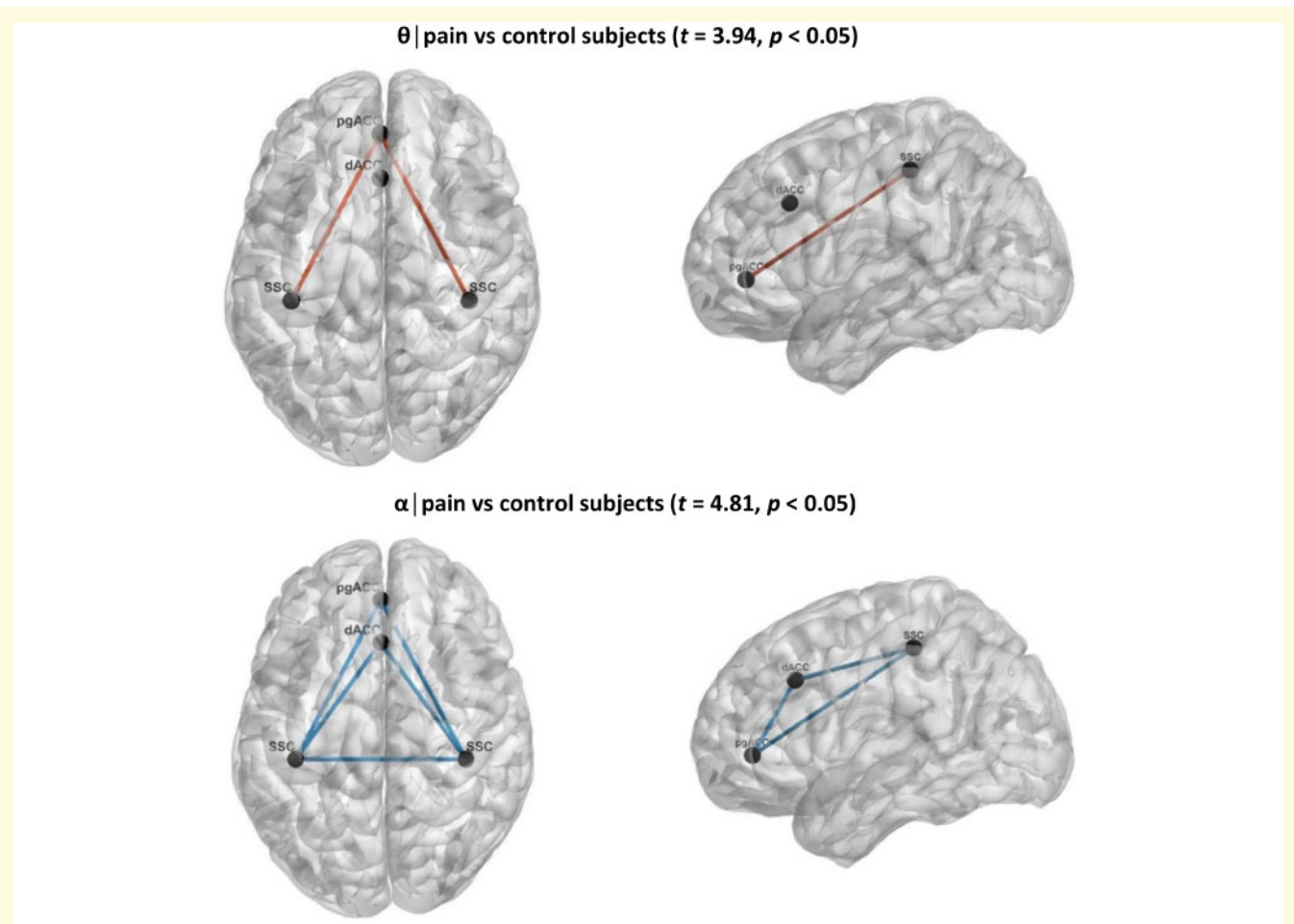


Figure 2 Functional connectivity in pain. Functional connectivity between patients with chronic pain in comparison to control subjects shows a significant change in the θ and α frequency band. For θ , a significant increase in functional connectivity was revealed between the pgACC and the left and right SSC for chronic pain patients, while for α a decreased functional connectivity was revealed between the pgACC, dACC and the left and right SSC for chronic pain patients.

No effect was obtained for the information that is sent from the left SSC ($R^2 = 0.01$, $P = 0.52$) and right SSC ($R^2 = 0.03$, $P = 0.11$) to pgACC. For pain distress, no significant correlations were obtained for pgACC to the left ($R^2 = 0.0001$, $P = 0.99$) and right SSC ($R^2 = 0.001$, $P = 0.91$) or from left SSC ($R^2 = 0.02$, $P = 0.88$) and right SSC ($R^2 = 0.02$, $P = 0.39$) to pgACC.

For the α band, an overall effect for the effective connectivity as measured with Granger causality was identified between the pgACC, dACC and the SSC ($F=4.70$, $P < 0.001$). A post-hoc univariate analysis indicated a significant increase ($F=5.81$, $P = 0.018$) in information flow from the dACC to the pgACC for pain patients ($M = 0.021$, $SD = 0.011$) in comparison to control subjects ($M = 0.015$, $SD = 0.014$). From the pgACC to the dACC, we found a significant decrease ($F=22.48$, $P < 0.001$) in information flow for pain patients ($M = 0.013$, $SD = 0.008$) in comparison to control subjects ($M = 0.022$, $SD = 0.010$). Furthermore, the analysis yielded a significant decrease for information flow from the

pgACC to the left and right SCC for pain patients (left: $M = 0.006$, $SD = 0.0008$; $F=11.94$, $P = 0.001$; right: $M = 0.007$, $SD = 0.007$; $F=6.29$, $P = 0.014$) in comparison to control subjects (left: $M = 0.012$, $SD = 0.008$; right: $M = 0.010$, $SD = 0.009$). Univariate analyses revealed no effect for effective connectivity between the left SSC ($F = 0.14$, $P = 0.71$); and right SCC ($F = 0.037$, $P = 0.85$) to the pgACC. Also, for the left SSC ($F = 0.10$, $P = 0.76$); and right SCC ($F = 0.12$, $P = 0.74$) to dACC no effect was obtained. No effect was obtained for the dACC to the left SSC ($F = 0.06$, $P = 0.82$); and right SCC ($F = 0.05$, $P = 0.83$).

A correlation analysis revealed only a significant effect between pain intensity perception using the NRS and information flow from the dACC to the pgACC ($R^2 = 0.24$, $P < 0.001$), indicating that the more pain was perceived by patients, the more information flowed from the dACC to the pgACC. No correlation was obtained for the pain percept and information flow from the pgACC to the dACC ($R^2 = 0.01$, $P = 0.90$), from the pgACC to

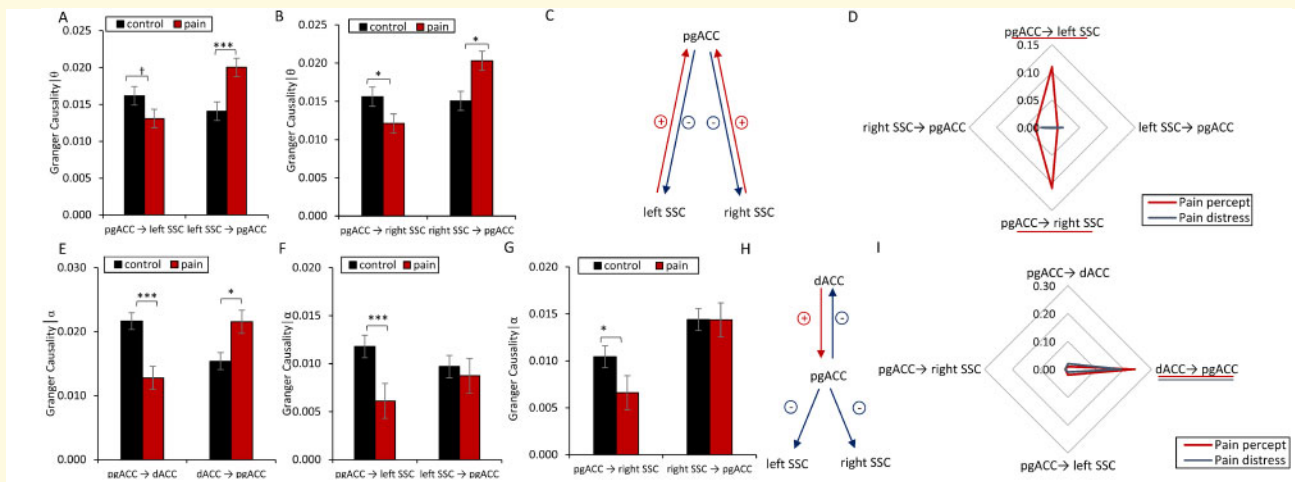


Figure 3 Effective connectivity in pain. (A–C) For the θ frequency band, a decrease in effective connectivity from the pregenual anterior cingulate cortex (pgACC) to the left and right the left and right somatosensory cortex (SSC) was identified, while an increase in effective connectivity from the left and right the left and right SSC to the pgACC was found for chronic pain patients in comparison to controls subjects. (D) A correlation analysis between pain intensity perception the left and right SSC to pgACC demonstrates that more pain is related to less effective connectivity in chronic pain patients. (E–H) For the α frequency band, a decrease in effective connectivity from the pgACC to the left and right SSC as well as the dorsal anterior cingulate cortex (dACC) was found for chronic pain patients. In contrast, no difference in effective connectivity from the left and right SSC to the dACC to the pgACC was noted for chronic pain patients in comparison to controls subjects. (I) A positive correlation was identified between pain perception with effective connectivity from dACC to pgACC, indicating the higher pain intensities and distress correlate with increased effective connectivity from dACC to pgACC in chronic pain patients. No effect was obtained for the effective connectivity from pgACC to SCC (left and right) or from pgACC to dACC. ($\dagger P < 0.10$, $*P < 0.05$, $**P < 0.01$, $***P < 0.001$). For the radar plots, effective connectivity areas underlined indicate a significant effect (blue for pain distress, red for pain intensity).

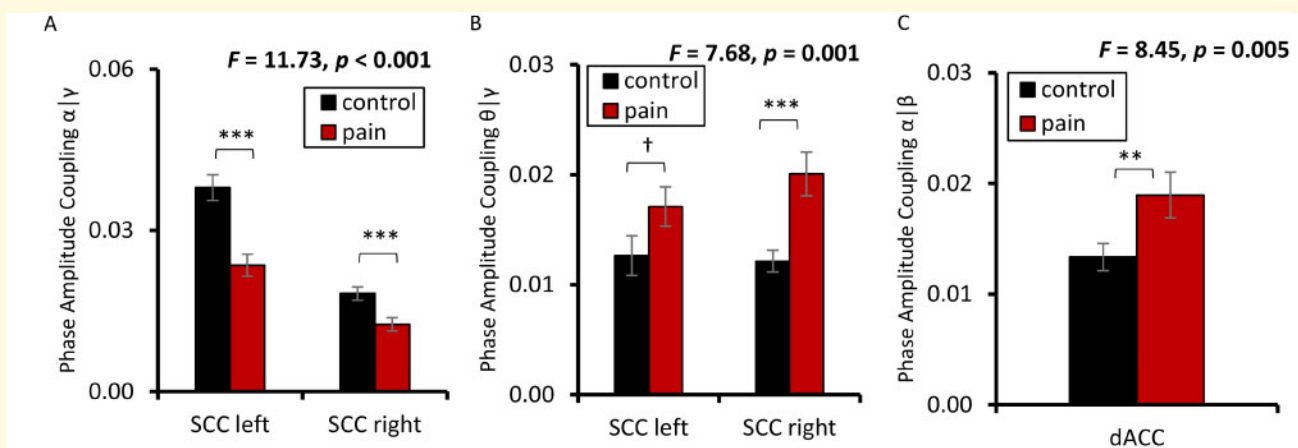


Figure 4 Cross-frequency coupling in pain. A significant decrease in α - γ coupling (a) and a significant increase in θ - γ coupling (b) was obtained for the left and right SCC for patients with chronic pain in comparison to control subjects. For the dACC, an increase in α - β coupling (c) was found for patients with chronic pain in comparison to control subjects. ($\dagger P < 0.10$, $*P < 0.05$, $**P < 0.01$, $***P < 0.001$).

the left SSC ($R^2 = 0.02$, $P = 0.58$) or from the pgACC to the right SSC ($R^2 = 0.01$, $P = 0.52$), respectively. For pain distress, only a significant correlation was obtained between pain distress and information flow from the dACC to the pgACC ($R^2 = 0.19$, $P = 0.002$). No correlation was obtained for the pain distress and information flow from the pgACC to the dACC ($R^2 = 0.02$, $P = 0.39$), from the pgACC to the left SSC ($R^2 = 0.01$, $P =$

0.50) or from the pgACC to the right SSC ($R^2 = 0.01$, $P = 0.53$), respectively. The effect remained after correction for multiple comparison using a Bonferroni correction.

Phase amplitude coupling

For θ - γ coupling, a significant difference was obtained for the left and right SSC ($F = 7.68$, $P < 0.001$) between

pain patients and control subjects. A post-hoc univariate analysis, revealed for right SSC ($M = 0.020$, $SD = 0.012$; $F = 14.64$, $P < 0.001$) increased θ - γ coupling for pain patients in comparison to control subjects ($M = 0.012$, $SD = 0.008$). For the left SSC ($M = 0.017$, $SD = 0.008$; $F = 2.91$, $P = 0.091$), there was only a marginally significant increase in θ - γ coupling for the pain patients in comparison to control subjects ($M = 0.012$, $SD = 0.009$ (Fig. 4a-c)).

No correlation was obtained between the pain intensity percept and θ - γ coupling for the left SSC ($R^2 = 0.03$, $P = 0.25$) and right SSC ($R^2 = 0.002$, $P = 0.79$). For pain distress, no correlation was obtained with θ - γ coupling for the left SSC ($R^2 = 0.01$, $P = 0.87$) and right SSC ($R^2 = 0.001$, $P = 0.90$).

For α - β coupling, a significant effect SSC ($F = 10.22$, $P < 0.001$) was obtained of the dACC when comparing pain patients ($M = 0.018$, $SD = 0.009$) in comparison to control subjects ($M = 0.013$, $SD = 0.008$). No correlation was obtained between the pain percept and θ - γ coupling for ($R^2 = 0.001$, $P = 0.95$) or between pain distress and θ - γ coupling ($R^2 = 0.001$, $P = 0.80$) for the dACC.

Discussion

This study provides converging evidence that chronic pain is an imbalance between brain areas involved in ascending and descending pain pathways. This imbalance is controlled by different brain oscillations that all contribute in routing of information flow between brain areas involved in pain input and pain suppression (Ploner *et al.*, 2017).

This study confirms that chronic pain is associated with increased θ and γ oscillations in the SSC, the main hub of the lateral ‘painfulness’ pathway, in agreement with the thalamocortical dysrhythmia model (Llinas *et al.*, 1999; Vanneste *et al.*, 2018), and specifies γ band activity in the somatosensory cortex correlates with intensity of chronic pain, similar to what is noted in acute experimental pain (Babiloni *et al.*, 2002).

The dACC, as main hub of the medial ‘suffering’ pathway, accelerates from θ to α and β frequencies, also suggesting an increase in pain processing.

The descending pain inhibitory system with the pgACC as main hub, which normally oscillates at rest in θ (Vanneste *et al.*, 2019). The results of this study demonstrate that the descending pain inhibitory system accelerates from θ to α suggesting that pain suppression is paradoxically increased, possibly as an attempt, albeit insufficient, to compensate for the increase in pain input. This strongly suggests that indeed a balance better explains pain than only pain input.

The imbalance can improve either by reducing pain input or increasing pain suppression. Spinal cord stimulation seems to rely on increased pgACC activity (Moens

et al., 2012), and by increasing pain suppression rebalancing pain suppression with pain input (De Ridder and Vanneste, 2016, 2017). This not only seems to be the main mechanism of action of spinal cord stimulation, but of motor cortex stimulation (Lima and Fregni, 2008). But also opioids (Fields, 2004) and SNRIs such as duloxetine (Lunn *et al.*, 2009; Kremer *et al.*, 2018) exert their pain suppressing effects by modulation of the descending pain inhibitory system. Furthermore, if the descending pain inhibitory system is deficient, as in fibromyalgia, people perceive generalized pain (Jensen *et al.*, 2013).

A balance, by definition, requires communication between pain input and suppression between the dACC, SSC, and pgACC. Thus, the lack of communication, as demonstrated by decreased functional connectivity between pain input and pain suppression, results in a loss of balance between interacting areas. Indeed, the results of this study indicate functional connectivity changes between dACC, SSC, and pgACC for both the θ and α band. A closer look at the data by analyzing effective connectivity indicates that for the θ band, less information is sent from the pgACC to the left and right SSC. This finding is associated with increased pain and fits with the idea that the imbalance is due to reduced pain suppression. For α , increased information is sent from the dACC to the pgACC, which correlates with the intensity of the pain percept. This latter finding could suggest that the dACC is inhibiting activity in the pgACC, explaining the reduced information being sent from the pgACC to the dACC, and the left and right SSC. Conceptually, the brain attaches a paradoxical behavioural significance to the pain percept, by which it remains conscious. Indeed fluctuations of the salience network results in conscious perception of somatosensory stimuli at threshold (Boly *et al.*, 2007). Furthermore, it has been shown that all psychosurgical interventions ultimately result in modulation of the pgACC (Schoene-Bake *et al.*, 2010). Thus a dACC cingulotomy will reduce the dACC part of the ratio, possibly normalizing the imbalance by releasing the pgACC from inhibitory activity (De Ridder *et al.*, 2016). And cingulotomies have been successfully used to treat chronic pain (Wilkinson *et al.*, 1999; Cetas *et al.*, 2008; Yen *et al.*, 2009).

The findings of this study also identify increased θ - γ coupling in the SSC, which is consistent with the thalamocortical dysrhythmia model of pain that proposes that α - γ nesting is a physiological mechanism transmitting sensory information and that slowed down alpha into the θ range reflects pathological θ - γ coupling, associated with tinnitus and pain (Llinas *et al.*, 1999; De Ridder *et al.*, 2015).

The balance disorder also suggests that there are multiple ways the brain can generate pain, either related to too much pain input, or because of deficient pain suppression, or a combination of the two. This could benefit a new brain-based classification of different types of

pain, rather than the traditional etiology-based categorization of pain and may help to develop a mechanism-based approach for selecting therapy. Indeed, fibromyalgia pain has been attributed to a deficiency in pain suppression (Jensen *et al.*, 2013) and a balance problem between pain input and pain suppression (De Ridder and Vanneste, 2017), and this imbalance can be normalized by occipital nerve field stimulation (De Ridder and Vanneste, 2017). It is of interest that this imbalance mechanism might be more universal in view of the pathophysiological analogy between pain, tinnitus, Parkinson's disease and major depression (Llinas *et al.*, 1999; Vanneste *et al.*, 2018) as well as reward-deficiency disorders, such as obesity, addiction, hyperactivity and personality disorders (Blum *et al.*, 2014). Indeed, the described mechanism involves the same brain areas involved in reward-deficiency disorders, resulting from allostasis, i.e. reference resetting (De Ridder *et al.*, 2016).

Furthermore, the fact that pain can be detected by machine learning with 89.3% accuracy, and if this concept is generalizable, will permit to develop objective measures for other subjective states such as tinnitus, depression, anxiety by measuring ratios of current density in the hubs that drive the ascending and descending pathways, rather than measuring electrical activity of only input areas of sensory pathways as was routinely done in for example tinnitus (van der Loo *et al.*, 2009), pain (Babiloni *et al.*, 2002) and depression (Jaworska *et al.*, 2012). The imbalance theory also permits to more rationally prescribe medications by clinicians. For example, combining medication that activate pain inhibition, with medications that inhibit pain input will be more effective in rebalancing pain or tinnitus or depression states than medication that only addresses one of the pain pathways. Thus, the magic bullet concept of Nobel laureate Paul Ehrlich (Winau *et al.*, 2004) does not hold in this concept, except if one medication would simultaneously modulate all three pathways. Ehrlich envisioned that just like a bullet fired from a gun aiming to hit a specific target, there must be a pharmacological way to specifically target a symptom or disease, in his case invading microbes. A more rational pain treatment however is to combine a drug that activates the descending pain inhibitory pathway, with another one that suppresses the medial pathway and a third that suppresses the lateral pathway. This cocktail approach is similar to what is very successfully used in for example AIDS pharmacotherapy, keeping the disease under control in 85–90% of patients (Lu *et al.*, 2018).

Although chronic pain is one of the most important medical problems facing society, there has been limited progress in finding an objective measure for this fundamentally subjective state. A conceptually new way of defining pain electrophysiologically may aid in developing better subtyping, better diagnostic measures and better treatments for chronic pain.

In conclusion, this paper presents a fundamentally new concept of pain as an imbalance disorder in the brain, which may have large implications, not only as a basis for finding an objective measure for a subjective pain state, but also for developing better pain medication, novel neurostimulation designs, and subtyping pain. Furthermore, in view of the analogy of the underlying pathophysiology of pain, tinnitus, depression, Parkinson's disease (Vanneste *et al.*, 2018), and slow wave epilepsy (Llinas *et al.*, 1999), there is no reason to believe this concept could not be extended to other subjective states.

Funding

No funding.

Competing interests

The authors of no conflict of interests related to this research.

References

- Babiloni C, Babiloni F, Carducci F, Cincotti F, Rosciarelli F, Arendt-Nielsen L, et al. Human brain oscillatory activity phase-locked to painful electrical stimulations: a multi-channel EEG study. *Hum Brain Mapp* 2002; 15: 112–23.
- Blum K, Oscar-Berman M, Demetrovics Z, Barh D, Gold MS. Genetic Addiction Risk Score (GARS): molecular neurogenetic evidence for predisposition to Reward Deficiency Syndrome (RDS). *Mol Neurobiol* 2014; 50: 765–96.
- Boly M, Baeteau E, Schnakers C, Degueldre C, Moonen G, Luxen A, et al. Baseline brain activity fluctuations predict somatosensory perception in humans. *Proc Natl Acad Sci U S A* 2007; 104: 12187–92.
- Bushnell MC, Čeko M, Low LA. Cognitive and emotional control of pain and its disruption in chronic pain. *Nat Rev Neurosci* 2013; 14: 502–11.
- Canolty RT, Edwards E, Dalal SS, Soltani M, Nagarajan SS, Kirsch HE, et al. High gamma power is phase-locked to theta oscillations in human neocortex. *Science* 2006; 313: 1626–8.
- Cauda F, Sacco K, D'Agata F, Duca S, Cocito D, Geminiani G, et al. Low-frequency BOLD fluctuations demonstrate altered thalamocortical connectivity in diabetic neuropathic pain. *BMC Neurosci* 2009; 10: 138.
- Cetas JS, Saedi T, Burchiel KJ. Destructive procedures for the treatment of nonmalignant pain: a structured literature review. *JNS* 2008; 109: 389–404.
- Coullaut-Valera R, Arbaiza I, Bajo R, Arrue R, Lopez ME, Coullaut-Valera J, et al. Drug polyconsumption is associated with increased synchronization of brain electrical-activity at rest and in a counting task. *Int J Neural Syst* 2014; 24: 1450005.
- De Ridder D, Manning P, Leong SL, Ross S, Vanneste S. Allostasis in health and food addiction. *Sci Rep* 2016; 6: 37126.
- De Ridder D, van der Loo E, Vanneste S, Gais S, Plazier M, Kovacs S, et al. Theta-gamma dysrhythmia and auditory phantom perception. *JNS* 2011; 114: 912–21.
- De Ridder D, Vanneste S. Burst and tonic spinal cord stimulation: different and common brain mechanisms. *Neuromodulation* 2016; 19: 47–59.
- De Ridder D, Vanneste S. Occipital nerve field transcranial direct current stimulation normalizes imbalance between pain detecting and

- pain inhibitory pathways in fibromyalgia. *Neurotherapeutics* 2017; 14: 484–501.
- De Ridder D, Vanneste S, Gillett G, Manning P, Glue P, Langguth B. Psychosurgery reduces uncertainty and increases free will? A review. *Neuromodulation* 2016; 19: 239–48.
- De Ridder D, Vanneste S, Langguth B, Llinas R. Thalamocortical dysrhythmia: a theoretical update in tinnitus. *Front Neurol* 2015; 6: 124
- de Vries M, Wilder-Smith OH, Jongasma ML, van den Broeke EN, Arns M, van Goor H, et al. Altered resting state EEG in chronic pancreatitis patients: toward a marker for chronic pain. *J Pain Res* 2013; 6: 815–24.
- Eippert F, Bingel U, Schoell ED, Yacubian J, Klinger R, Lorenz J, et al. Activation of the opioidergic descending pain control system underlies placebo analgesia. *Neuron* 2009; 63: 533–43.
- Fields H. State-dependent opioid control of pain. *Nat Rev Neurosci* 2004; 5: 565–75.
- Flor H, Elbert T, Knecht S, Wienbruch C, Pantev C, Birbaumer N, et al. Phantom-limb pain as a perceptual correlate of cortical reorganization following arm amputation. *Nature* 1995; 375: 482–4.
- Fuchs M, Kastner J, Wagner M, Hawes S, Ebersole JS. A standardized boundary element method volume conductor model. *Clin Neurophysiol* 2002; 113: 702–12.
- Gaskin DJ, Richard P. The economic costs of pain in the United States. *J Pain* 2012; 13: 715–24.
- Geweke J. Measurement of linearity dependence and feedback between multiple time series. *J Am Stat Assoc* 1982; 77: 304–13.
- Granger CWJ. Investigating causal relations by econometrics models and cross-spectral methods. *Econometrica* 1969; 37: 424.
- Jaworska N, Blier P, Fusee W, Knott V. Alpha power, alpha asymmetry and anterior cingulate cortex activity in depressed males and females. *J Psychiatr Res* 2012; 46: 1483–91.
- Jensen KB, Srinivasan P, Spaeth R, Tan Y, Kosek E, Petzke F, et al. Overlapping structural and functional brain changes in patients with long-term exposure to fibromyalgia pain. *Arthritis Rheum* 2013; 65: 3293–303.
- Jensen MP, Day MA, Miro J. Neuromodulatory treatments for chronic pain: efficacy and mechanisms. *Nat Rev Neurol* 2014; 10: 167–78.
- Jensen MP, Sherlin LH, Gertz KJ, Braden AL, Kupper AE, Ganas A, et al. Brain EEG activity correlates of chronic pain in persons with spinal cord injury: clinical implications. *Spinal Cord* 2013; 51: 55–8.
- Jurcak V, Tsuzuki D, Dan I. 10/20, 10/10, and 10/5 systems revisited: their validity as relative head-surface-based positioning systems. *Neuroimage* 2007; 34: 1600–11.
- Kim JW, Kim SY, Choi JW, Kim KM, Nam SH, Min KJ, et al. Differences in resting-state quantitative electroencephalography patterns in attention deficit/hyperactivity disorder with or without comorbid symptoms. *Clin Psychopharmacol Neurosci* 2017; 15: 138–45.
- Kim JW, Lee J, Kim HJ, Lee YS, Min KJ. Relationship between theta-phase gamma-amplitude coupling and attention-deficit/hyperactivity behavior in children. *Neurosci Lett* 2015; 590: 12–7.
- Kong J, Loggia ML, Zyloney C, Tu P, Laviolette P, Gollub RL. Exploring the brain in pain: activations, deactivations and their relation. *Pain* 2010; 148: 257–67.
- Kremer M, Yalcin I, Goumon Y, Wurtz X, Nexon L, Daniel D, et al. A dual noradrenergic mechanism for the relief of neuropathic allodynia by the antidepressant drugs duloxetine and amitriptyline. *J Neurosci* 2018; 38: 9934–54.
- Lima MC, Fregni F. Motor cortex stimulation for chronic pain: systematic review and meta-analysis of the literature. *Neurology* 2008; 70: 2329–37.
- Lisman JE, Jensen O. The theta-gamma neural code. *Neuron* 2013; 77: 1002–16.
- Llinas R, Urbano FJ, Leznik E, Ramirez RR, van Marle HJ. Rhythmic and dysrhythmic thalamocortical dynamics: GABA systems and the edge effect. *Trends Neurosci* 2005; 28: 325–33.
- Llinas RR, Ribary U, Jeanmonod D, Kronberg E, Mitra PP. Thalamocortical dysrhythmia: a neurological and neuropsychiatric syndrome characterized by magnetoencephalography. *Proc Natl Acad Sci U S A* 1999; 96: 15222–7.
- Logan JM, Sanders AL, Snyder AZ, Morris JC, Buckner RL. Under-recruitment and nonselective recruitment: dissociable neural mechanisms associated with aging. *Neuron* 2002; 33: 827–40.
- Lu DY, Wu HY, Yarla NS, Xu B, Ding J, Lu TR. HAART in HIV/AIDS treatments: future trends. *Infect Disord Drug Targets* 2018; 18: 15–22.
- Lunn MP, Hughes RA, Wiffen PJ. Duloxetine for treating painful neuropathy or chronic pain. *Cochrane Database Syst Rev* 2009; CD007115.
- Moazami-Goudarzi M, Michels L, Weisz N, Jeanmonod D. Temporo-insular enhancement of EEG low and high frequencies in patients with chronic tinnitus. QEEG study of chronic tinnitus patients. *BMC Neurosci* 2010; 11: 40.
- Moens M, Sunaert S, Marien P, Brouns R, De Smedt A, Droogmans S, et al. Spinal cord stimulation modulates cerebral function: an fMRI study. *Neuroradiology* 2012; 54: 1399–407.
- Mumtaz W, Vuong PL, Xia L, Malik AS, Rashid RBA. An EEG-based machine learning method to screen alcohol use disorder. *Cogn Neurodyn* 2017; 11: 161–71.
- Pascual-Marqui R, (2007a). Discrete, 3D distributed, linear imaging methods of electric neuronal activity. Part 1: exact, zero error localization. <https://arxiv.org/abs/0710.3341> (23 February 2021, date last accessed).
- Pascual-Marqui R, (2007b). Instantaneous and lagged measurements of linear and nonlinear dependence between groups of multivariate time series: frequency decomposition. <https://arxiv.org/abs/0711.1455> (23 February 2021, date last accessed).
- Pascual-Marqui RD. Standardized low-resolution brain electromagnetic tomography (sLORETA): technical details. *Methods Find Exp Clin Pharmacol* 2002; 24 Suppl D: 5–12.
- Ploner M, Sorg C, Gross J. Brain rhythms of pain. *Trends Cogn Sci* 2017; 21: 100–10.
- Price DD. Psychological and neural mechanisms of the affective dimension of pain. *Science* 2000; 288: 1769–72.
- Rainville P, Duncan GH, Price DD, Carrier B, Bushnell MC. Pain affect encoded in human anterior cingulate but not somatosensory cortex. *Science* 1997; 277: 968–71.
- Roelofs J, Peters ML, McCracken L, Vlaeyen JW. The pain vigilance and awareness questionnaire (PVAQ): further psychometric evaluation in fibromyalgia and other chronic pain syndromes. *Pain* 2003; 101: 299–306.
- Sametsky EA, Turner JG, Larsen D, Ling L, Caspary DM. Enhanced GABAA-mediated tonic inhibition in auditory thalamus of rats with behavioral evidence of tinnitus. *J Neurosci* 2015; 35: 9369–80.
- Sarnthein J, Morel A, von Stein A, Jeanmonod D. Thalamocortical theta coherence in neurological patients at rest and during a working memory task. *Int J Psychophysiol* 2005; 57: 87–96.
- Sarnthein J, Stern J, Aufenberg C, Rousson V, Jeanmonod D. Increased EEG power and slowed dominant frequency in patients with neurogenic pain. *Brain* 2006; 129: 55–64.
- Schmidt S, Naranjo JR, Brenneisen C, Gundlach J, Schultz C, Kaube H, et al. Pain ratings, psychological functioning and quantitative EEG in a controlled study of chronic back pain patients. *PLoS One* 2012; 7: e31138.
- Schoene-Bake JC, Parpaley Y, Weber B, Panksepp J, Hurwitz TA, Coenen VA. Tractographic analysis of historical lesion surgery for depression. *Neuropsychopharmacology* 2010; 35: 2553–63.
- Schulman JJ, Cancro R, Lowe S, Lu F, Walton KD, Llinas RR. Imaging of thalamocortical dysrhythmia in neuropsychiatry. *Front Hum Neurosci* 2011; 5: 69
- Siepmann M, Kirch W. Effects of caffeine on topographic quantitative EEG. *Neuropsychobiology* 2002; 45: 161–6.
- Smith TC, Frank E. Introducing machine learning concepts with WEKA. In: Mathe E, Davis S, editors. *Statistical genomics: methods and protocols*. New York, USA: Springer; 2016. p. 348–353.

- Song JJ, Vanneste S, De Ridder D. Dysfunctional noise cancelling of the rostral anterior cingulate cortex in tinnitus patients. *PLoS One* 2015; 10: e0123538.
- Stern J, Jeanmonod D, Sarnthein J. Persistent EEG overactivation in the cortical pain matrix of neurogenic pain patients. *Neuroimage* 2006; 31: 721–31.
- Treede RD, Rief W, Barke A, Aziz Q, Bennett MI, Benoliel R, et al. A classification of chronic pain for ICD-11. *Pain* 2015; 156: 1003–7.
- van der Loo E, Gais S, Congedo M, Vanneste S, Plazier M, Menovsky T, et al. Tinnitus intensity dependent gamma oscillations of the contralateral auditory cortex. *PLoS One* 2009; 4: e7396.7391–7395.
- Vanneste S, Alsalman O, De Ridder D. Top-down and bottom-up regulated auditory phantom perception. *J Neurosci* 2019; 39: 364–78.
- Vanneste S, Congedo M, De Ridder D. Pinpointing a highly specific pathological functional connection that turns phantom sound into distress. *Cereb Cortex* 2014; 24: 2268–82.
- Vanneste S, Song JJ, De Ridder D. Thalamocortical dysrhythmia detected by machine learning. *Nat Commun* 2018; 9: 1103.
- Volkow ND, Logan J, Fowler JS, Wang GJ, Gur RC, Wong C, et al. Association between age-related decline in brain dopamine activity and impairment in frontal and cingulate metabolism. *Am J Psychiatry* 2000; 157: 75–80.
- Walton KD, Dubois M, Llinas RR. Abnormal thalamocortical activity in patients with Complex Regional Pain Syndrome (CRPS) type I. *Pain* 2010; 150: 41–51.
- Wilkinson HA, Davidson KM, Davidson RI. Bilateral anterior cingulotomy for chronic noncancer pain. *Neurosurgery* 1999; 45: 1129–34. discussion 1134–1126.
- Winau F, Westphal O, Winau R. Paul Ehrlich—in search of the magic bullet. *Microbes Infect* 2004; 6: 786–9.
- Yen CP, Kuan CY, Sheehan J, Kung SS, Wang CC, Liu CK, et al. Impact of bilateral anterior cingulotomy on neurocognitive function in patients with intractable pain. *J Clin Neurosci* 2009; 16: 214–9.
- Yilmaz P, Diers M, Diener S, Rance M, Wessa M, Flor H. Brain correlates of stress-induced analgesia. *Pain* 2010; 151: 522–9.